

# A new approach to develop biometric fingerprint using human right thumb fingernail

Tahani Ghanim Al-Sultan<sup>1</sup>, Aza Qays Abduljabar<sup>1</sup>, Warqaa Hashim Alkhalel<sup>1</sup>,  
Zaid Husham Al-Sawaff<sup>1,2</sup>, Fatma Kandemirli<sup>3</sup>

<sup>1</sup>Technical Engineering College, Northern Technical University (NTU), Mosul, Iraq

<sup>2</sup>Center of Technical Research, Northern Technical University (NTU), Mosul, Iraq

<sup>3</sup>Department of Biomedical Engineering, Faculty of Engineering and Architecture, Kastamonu University, Kastamonu, Turkey

## Article Info

### Article history:

Received Sep 11, 2022

Revised Mar 24, 2023

Accepted Mar 28, 2023

### Keywords:

Biometric authentication

Fingernails

Lunula

Nail plate

Semantic points

## ABSTRACT

In this article, we analyzed the structure of human nails to develop a modern biometric authentication system based on the nail bed and finger lunula. The results of the studies on the collected images proved that each fingernail has distinctive characteristics in terms of the length and width of the nail and the lunula, even identical twins. We focused on the fingernail of the right thumb because of its large size and the accuracy and clarity of the nail. The mediation of the indicative points on the nail bed and on the lunula was used to form the pentagonal structure and use it as a region of interest. Then an ensemble independent component analysis, principal component analysis, haar wavelet, and scale invariant feature transformation, were used. Later we classified these algorithms using support vector machine and Naive Bayes techniques, the performance of each algorithm was analyzed by feature extraction with two classifiers. This study was conducted on 100 participants and showed that this new method could be used as a biometric identification system for humans. There was no similarity in results for all verified samples.

This is an open access article under the [CC BY-SA](https://creativecommons.org/licenses/by-sa/4.0/) license.



## Corresponding Author:

Zaid Husham Al-Sawaff

Technical Engineering College, Northern Technical University (NTU)

Mosul, Iraq

Email: zaidalsawaff@ntu.edu.iq

## 1. INTRODUCTION

The biometric identification system can be defined as the most flexible and efficient way to identify or authenticate individuals [1], [2], as one of the main advantages of these systems is that the concerned person does not need to remember or write a password or carry a smart card, which leads to faster speed use and reduce password management costs.

Recently, many biometric technologies have been relied on, such as face or fingerprint, iris, ear print, hand geometry, and voice signature, to identify or authenticate identity. Still, there was a need to use other biometric authentication techniques such as lip print or joints or fingerprints to reduce the problems associated with previous techniques or speed up these modern systems' work [3]. Also, due to much previous research conducted on modern measurement techniques, which gave excellent results, these techniques can be adopted in identification or password systems and security and forensic systems.

Recently, researchers' efforts have focused on developing touchless acquisition systems to reduce the risk of attacks by fraudsters. These efforts focused on capturing vital features without touching depending on the unique characteristics that distinguish a human from others, such as joint engineering, nails, or hand engineering [3]. Anatomical studies of the nail show that the nail plate is the only one that regenerates with the production of new cells, as the spacing distance the nail grooves remains relatively constant throughout the life

of the nail. These grooves are of great importance and a high degree of distinction and difference, even identical twins and even the nails of the same hand [4]. For this purpose, the nail bed was relied on as a primary method for measuring changes in biometrics in this research. Figure 1 shows the anatomy of the human fingernail.

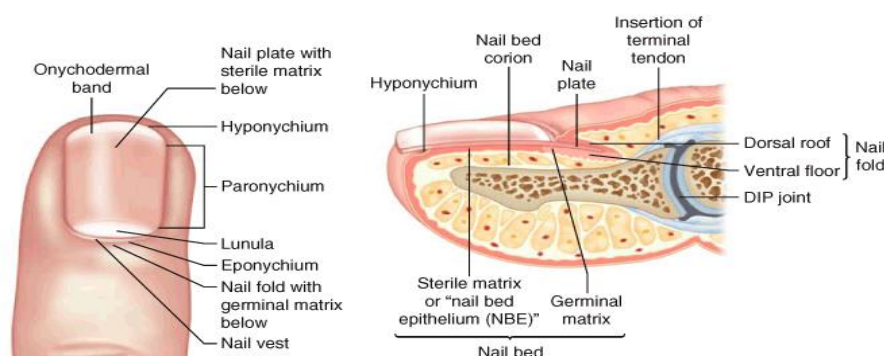


Figure 1. The fingernail typical sample, with nail anatomy

With age, the average person's shape and size of the nail plate remain constant, unlike other vital characteristics such as the face or the ear, as their size and shape change over time [5]. This unique property of the nail can be considered a key to developing biometric authentication systems based on nails. The lunula [6] is a white half-moon-shaped area that can be found in the proximal ends of the nails, which grows beyond the edge of the proximal nail fold [7]. The primary function of the lunula is to specify the shape of the nail plate [8]. The nail consists of a keratinous structure in a rectangular and transparent shape. The nail covers the nail bed is arched with longitudinal and transverse axes and has trilamellar fibers (dorsal, ventral, and central) [9]. This curvature is to enhance the resistance of the nail to mechanical stress. The dorsal and ventral fibers run transversely, while the central fibers run longitudinally. This unique variety increases the nail's resistance to fracturing and tearing [10], [11]. This research is organized as shown in: The section 1 contains the introduction and the research problem, while the section 2 describes some important literary reviews related to our research field. The section 3 discussed the proposed system and how it works. The experimental results are discussed in the section 4 of this paper. Finally, the section 5 concludes this research, presenting the final discussion with some future visions for the development of the research topic.

The subject of nail-based biometric validations is a recent topic, and for this reason, there is not a large number of literature reviews on this topic. This section will review the most important of what came in some of these reviews, which are related to the biometric authentication systems. Barbosa *et al.* [12] proposed the concept of transient biometrics, and this concept is one of the most current concepts used to identify some biometrics. The authors focused on established vital characteristics and used the nail as a case study. They relied on extracting images of fingernails using different texture features. The obtained results proved that the photos taken were reliable for one month from the date of their capture only because of the changes in the tissue on which the samples were taken. Therefore, this research was considered suitable for measuring transient vital activities only. On the other hand, Garg *et al.* [13] proposed an automated biometric authentication approach using fingernails and based on the back view of the hand and three fingers of one hand (ring, index, and middle). In this project, the nail plate was neglected, and the area called the nail bed was extracted based on the grayscale values the color of the nail skin, the implanted nail plate, and the nail bed. It was found that the value of the gray hue of the skin is lower than it is in the nail bed. The nail bed is extracted from the nail surface, relying on Haar wavelet feature extraction technology. No need to use a complex region of interest extraction (ROI) extraction algorithm. The proposed new system gave less accurate validation results than systems that use a single surface of the nail.

At the same time, Michael *et al.* [14] proposed a system to recognize the fingerprint without touching the device to the hand, relying on low-resolution cameras to take a picture of the user's hand to identify it. The ROI technique was used to track the image of the hand and extract the preset points of interest for the palm-based technique on applying the local bimodal texture descriptor low back pain (LBP) to the gradient responses the direction of printing. The experiments showed promising results on this subject, especially when using modified probabilistic neural networks (PNN) to match the features, and the fingerprint verification period did not exceed one second for each scan.

In 2013, Alghamdi *et al.* [15] proposed a new way to combine the features of the nails and the fingers joints simultaneously, as joint biometrics were combined with other biometrics of the fingers, which are unique

features of each person. This work was done by relying on an algorithm to extract ROI from joints and nails simultaneously, as four fingers of the same hand were relied upon, and the thumb was neglected. This system extracted finger joint features using mill frequency cepstral coefficient (MFCC) technique, and nail characteristics were extracted from second-level wavelet decomposition. The said parts were combined using feature-level fusion back-propagation neural network feeding. What is defective about this system is that it did not consider the nail plate, but it relied only on instantaneous images taken, which will lead to its failure in the future. To the authors' knowledge, the nail lunula has not been previously relied upon to make any measurement related to biometric authentication applications, considering that the nail lunula has advantages that differ from one person to another according to the studies and statistics studied.

## 2. METHOD

### 2.1. Data collection

Information about the nail bed and the lunula was taken from the right thumb of all study cases. This is because the nail bed information and the lunula are distinctive and unique. The system used to extract features is designed to operate on the nail bed on one side and the lunula on the other side, without reference to the developing nail plate because it is not continuous all the time. The new technique used relied on extracting the area formed out of five indicative points drawn on the nail bed and five other indicative points marked on the nail lunula and considering these two areas as a return on investment to extract the features. Figure 2 shows the total flow formula for the proposed system.

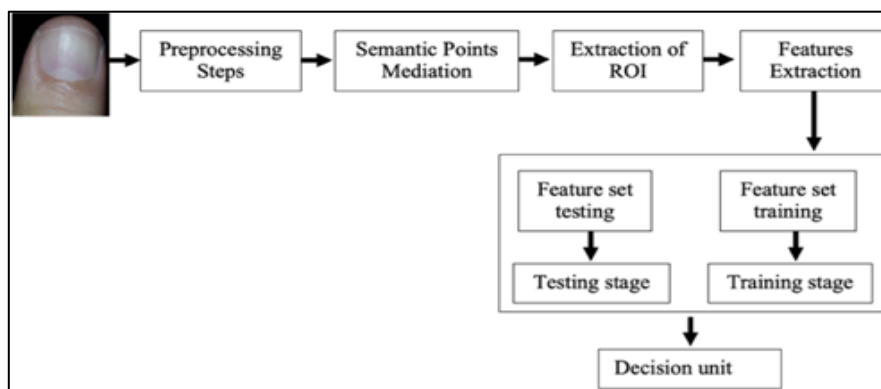


Figure 2. The proposed flowchart

### 2.2. Thumb image preprocessing

To get the best possible image taken, several modifications were made to the images using image processing techniques as follows: We first applied a 5×5 median filter mask [16] to remove random noise resulting from uneven lighting on the image. In the second stage, the Gabor filter [17], [18] was used to detect the edges of the image, as this type of filter has the maximum possible joint resolution in the spatial frequencies field. Researchers have frequently used this filter to develop the image and texture of an object or model. In the next stage, to obtain the highest possible contrast value, each image was subjected to the graph [19]. All obtained images are first optimized with a fixed threshold value. Then some shape repairs are made, such as filling in the holes inside the foreground shape, removing background debris, and finally connecting the edges of the finger image. In the final stage, we improve the essential features on the finger image using the Canny edge detection algorithm [20].

### 2.3. Conciliation of the semantic points

The nail bed cannot be accurately divided because the edges in the nail image are not continuous. For this, we used semantic point mediation techniques [21]. We have divided the work into steps for a direct understanding of the entire process. The first step paid attention to calculating the desired area using semantic point conciliation as in Figure 3. The perimeter of the nail lunula was calculated by its square as in Figure 3(a), and this was done by using the properties of the middle point [22]. Then, the same procedures were repeated to calculate the nail bed as in Figure 3(b). We create a common point on the nail bed and leave the nail plate in the second step. Then we rotated the image 180 degrees in order to perform the anterior process, and in this

way, the background of the image would be removed, and the color of the growing nail plate would be the same as the background color. For this, we ignored the nail plate. In the next stage, we draw a point at the end of the nail bed using two points, one at the base of the nail and the other at the end of the nail bed, and we connect them with a line called the super level line. Pixels were transferred from both ends of the nail using pixel mediation technology [23], and the point where both points intersect was marked as a central node point. These three points are easily distinguished in the binary image due to the pre-processing that has been done.

The final step is to draw the hyperplane [24], which is done by taking the length of the hyperplane and placing a vertical mark on the hyperplane at the center point of the node. Then we calculated the mediation of the semantic points based on the pixels from the central node region in the hyperplane and the intersection from the left and right regions until they reach the pixels of the edge region in the binary image. After we completed the process of finding the semantic points in the left and right regions, we took a quarter of the length of the hyperplane and moved the center point of the pixel up and down to get the midpoint; we connected the semantic points to form a pentagon and left the point at the base of the nail. At this point, the resulting nail image will appear after applying the semantic point mediation technique as in Figure 3(a). The texture properties of the resulting pentagon were masked, and this shape was used as a region of interest [25]. Next, we resized the extracted ROI to a size of 310×230 to extract the required features.

To increase the accuracy in performing the calculations, we repeated the same previous operations on the white area at the base of the nail, which is called the lunula as in Figure 3(b), where it was proven that each nail has its lunula representing one-fifth of the size of the nail which it varies from person to person [26]. Although the lunula is often not visible on all fingers, it is most consistently observed on the thumb [27]. In the same way, considered the lunula as a new independent nail as in Figure 3(b).

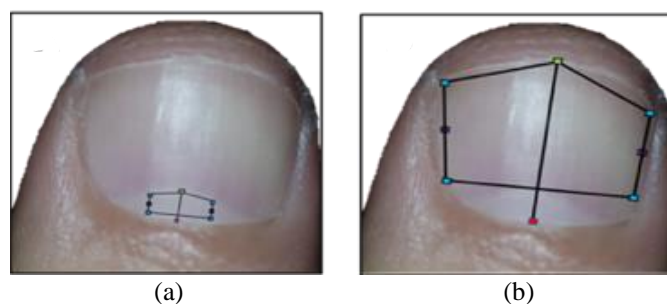


Figure 3. Choosing the desired area using semantic point conciliation: (a) the resulting image of the semantic point conciliation for the fingernail lunula and (b) semantic point mediation technique for the resulting fingernail image

## 2.4. Features of the extraction

The identification scheme proposed in this research depends mainly on the description of the nail tissue because the nail plate is mainly due to the unique texture of the nail. We used several methods to extract reliable features that distinguish different nail plates from their surfaces to apply biometrics in this paper. Discrete Haar functions may be defined as functions determined by sampling the Haar functions at  $2^n$  points. These functions can be conveniently represented by means of matrix form. The Haar matrices  $H(n)$  are considered in the natural and sequence ordering which differ in the ordering of rows. Each row of the matrix  $H(n)$  includes the discrete Haar sequence  $haar(w, t)$  (or otherwise the discrete Haar function). Independent component analysis (AIC) [28] are mathematical processes that filter mixed signals into subcomponent signals added to non-Gaussian signals. AIC represents the images obtained from input source as  $\{x_i(j), j=1, 2, \dots, n\}$ .

### 2.4.1. Haar wavelet

This waveform is considered one of the most direct waveforms compared to other types, as it provides information with great accuracy and satisfying about the image under test through the formation of the Haar-waveform pyramid [29], [30]. These waveforms can detect the differences different layers of tissue. The advantage of this method is that it is a non-continuous step and helps analyze images that suffer from spatial discontinuities. The primary wave of the Haar wave can be calculated and determined from (1) [29]–[31]:

$$\psi(t) = \begin{cases} 1 & 0 \leq t < \frac{1}{2} \\ -1 & \frac{1}{2} \leq t < 1 \\ 0 & \text{Otherwise} \end{cases} \quad (1)$$

the scaling function  $\varphi(t)$  is defined as [29].

$$\varphi(t) = \begin{cases} 1 & 0 \leq t < 1 \\ 0 & \text{Otherwise} \end{cases} \quad (2)$$

We generate a Haar Wavelet pyramid using the transformation application iteratively at low frequencies with an approximation of the nail image surface that gives a set of detailed parameters at each level. The image used for the nail surface was 230×310 with approximate diagonal, horizontal and vertical components. The five-level Haare waves gave high results, but what is wrong with them is that the higher level and the lower level give the highest accuracy and therefore cannot be distinguished them, so we chose to use the other three levels while ignoring the first and last levels to get the horizontal, vertical, and radial coefficients and they were used to form the attribute vectors [30].

#### 2.4.2. Analysis of independent components (AIC)

In this research, the AIC model considered the nail images as a set of independent models and relied on two matrices, the first is the mixing matrix let  $M_{N \times N}$ , and the second is the integrated circuit matrix for data matrices  $X_{k \times N}$  and using the given relationship in (3) [28], [32], [33] we get:

$$X_{k \times N} = C_{k \times N} \times M_{N \times N} \quad (3)$$

the function of AIC is to evaluate the independent components from the input images as [33]:

$$C = X \times M^{-1} \quad (4)$$

thus, defining C from X is known as blind source separation because the input source must be separated into independent components without any knowledge of the mixing matrix. We identified 32 independent components and stored them as AIC features for each column.

#### 2.4.3. Analysis of the components

The information from the nail bed contained strongly correlated data. Using the principal component analysis (PCA) method [34], we obtained less information because this method linked similar inputs by reducing the dimensions, and thus we reduced the amount of redundant information. After we change the size of the region of interest to 230×310, all the frames are compressed in that array and the form of its column representation, so we get a high amplitude value for each frame. One of the advantages of this method is that all frames are effectively identified, so it can be used to configure the attribute vector.

#### 2.4.4. Feature transformation of scale invariant SIFT

Scale invariant feature transform (SIFT) is an image descriptor for image-based matching and recognition developed by David Lowe (1999, 2004). This descriptor as well as related image descriptors are used for a large number of purposes in computer vision related to point matching different views of a 3-D scene and view-based object recognition. The SIFT descriptor is invariant to translations, rotations, and scaling transformations in the image domain and robust to moderate perspective transformations and illumination variations. Experimentally, the SIFT descriptor has been proven to be very useful in practice for image matching and object recognition under real-world conditions.

In its original formulation, the SIFT descriptor comprised a method for detecting interest points from a grey-level image at which statistics of local gradient directions of image intensities were accumulated to give a summarizing description of the local image structures in a local neighborhood around each interest point, with the intention that this descriptor should be used for matching corresponding interest points different images. Later, the SIFT descriptor has also been applied at dense grids (dense SIFT) which has been shown to lead to better performance for tasks such as object categorization, texture classification, image alignment, and biometrics. From the computer perspective, SIFT [35] detects and describes local features in an image so that any object in the image can extract distinct and exciting points and describe a unique feature of the object, that is, it can locate an object in an image that contains many other objects with many changes in scale image or noise and lighting in order to perform the required recognition, and these points are usually located in the high-

bay areas of any image. This paper used this technique as an input to the algorithm and to discover the feature points in the nail image.

### 3. RESULTS AND DESCUSSION

#### 3.1. The data set

In the current study, one hundred volunteers (fifty men and fifty women, with ten people of each sex the ages of twenties to sixties), no volunteer participated who have a history of injury or infection to their finger or toenail. We recorded details related to age, length of hands and fingers, and their proportion to body length to ensure that more information was collected in a standard position and an adequate assessment of the standard nail size.

To take the appropriate measurements, the previous studies were all taken into consideration, which included the best methods for measuring the length and width of the nail [36], [37], where the width of the nail ( $W$ ) was defined as the farthest transverse distance two points of the nail in the lateral groove. The length of the nail ( $L$ ) was defined as the furthest distance that can be measured the tip of the finger and the groove resulting from the intersection of the nail fold. Figure 4 illustrates the standard dimensions for the right thumb fingernail used in this article as a case study, where Figure 4(a) shows the end-on view of a fingernail, Figure 4(b) illustrates the lateral view of the fingernail, and Figure 4(c) showed the dorsal view of the fingernail. Also, to assess nail curvature, we measured the radius of the circle whose curvature approaches the nail plate, as shown in Figure 5. After that, the ratio of the length of the nail to its width was measured, and all the results were recorded to arrive at the final shape of the standard nail. One person took readings or calculations to avoid human errors during the measurement process. Table 1 shows all the parameters taken into considerations.

To study the effect of nail plate growth on the measurements, the data were divided into three main groups, where we applied the same acquisition process to the three groups. The first set ( $G1$ ) consists of photos of volunteer nails from the first acquisition day. At the same time, the second group ( $G2$ ) was composed of pictures of volunteer nails taken seven days after the initial acquisition. This group consisted of thirty individuals who were part of the first group ( $G1$ ). The third group ( $G3$ ) contained twenty-five images taken from the same volunteers in the second group ( $G2$ ), but sixty days after the initial acquisition. The results proved that nail plate growth did not affect the measurements taken or the validation mechanism, so we used the nail bed information to return on investment. Tables 2 and 3 explain the accuracy of the system algorithms used to extract the various features. Two classifiers were used to measure system accuracy, namely support-vector machine (SVM) [38] and Naive Bayes [39].

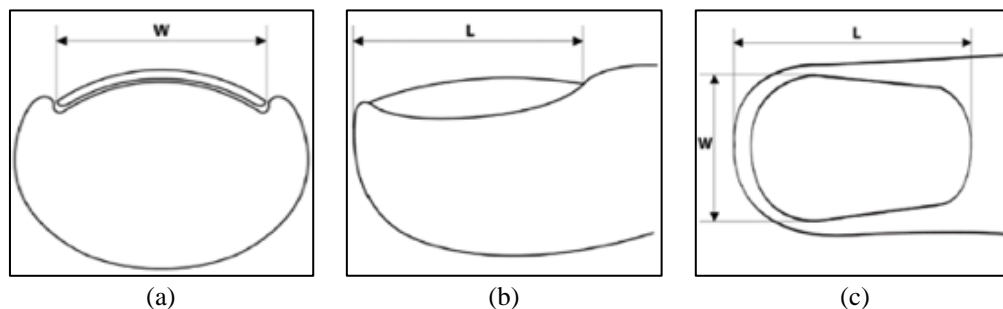


Figure 4. Fingernail dimentions using top and side views: (a) an end-on view of a fingernail, (b) a lateral view of the fingernail, and (c) a dorsal view of the fingernail

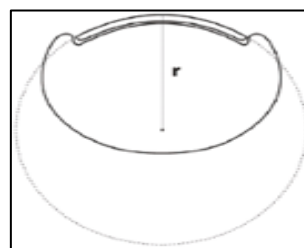


Figure 5. The radius of the circle drawn around the nail whose curve approximates the nail plate



In men, the mean age was  $45.8 \pm 14.2$  years, while in women, the mean age was  $45.3 \pm 13.8$  years. From the results observed, the length and width of the nail, the ratio of length to width, and the half diameter of the curvature of the nail were more considerable in men than it is in women. All these parameters had the most effective value in the thumb of both sexes, and the most significant value of the radius of curvature of the nails in the thumb was obtained for all cases studied and for both sexes.

Table 1. Thumb fingernail configurations for the investigated samples

Characteristic	Men	Women
Age (year)	$45.8 \pm 14.2$	$45.3 \pm 13.8$
Fingernail width (mm)	$14.8 \pm 1.0$	$12.9 \pm 1.1$
Fingernail length (mm)	$14.2 \pm 1.0$	$14.1 \pm 1.1$
Fingernail W/L ratio	$1.02 \pm 0.08$	$0.87 \pm 0.08$
The radius of transverse fingernail curvature (mm)	$11.2 \pm 1.3$	$9.4 \pm 0.8$

Table 2. Fingernails W/L ratio and the radius of transverse fingernails curvature for different age groups under investigation

Measurements	Age groups				
	20	30	40	50	60
	Men				
Thumb W/L ratio	$1.05 \pm 0.07$	$1.03 \pm 0.08$	$1.03 \pm 0.1$	$1.04 \pm 0.07$	$1.03 \pm 0.05$
The radius of transverse thumb curvature (mm)	$9.8 \pm 0.9$	$10.2 \pm 0.8$	$10.4 \pm 1.3$	$11.3 \pm 1.5g$	$11.3 \pm 1.4$
	Women				
Thumb W/L ratio	$0.91 \pm 0.08$	$0.91 \pm 0.09$	$0.91 \pm 0.1$	$0.91 \pm 0.06$	$0.92 \pm 0.05$
The radius of transverse fingernail curvature (mm)	$9.3 \pm 0.9$	$9.3 \pm 0.7$	$9.6 \pm 0.8$	$9.9 \pm 0.8$	$10.1 \pm 0.6$

Through the results obtained from all participants in the test, we found that the change in human age does not affect the ratio of nail length to width W/L, nor does it affect the nail bed. What should be noted is that the higher the person's age, the lower the radius of the nail curvature, meaning that the nails tend to flatten out as the person ages. This information was collected for statistical purposes only and to know the effect of age on the variables used in this research.

Table 3. Accuracy performance measurements

Feature extraction algorithm	Naive Bayes (%)	Support-vector machine SVM (%)
	Lunula	
Principal component analysis (PCA)	68.12	79.57
Analysis of independent components (AIC)	71.42	71.35
Haar wavelet	74.10	79.51
PCA+Haar	76.98	84.93
AIC+Haar	84.82	90.82
Feature transformation of scale-invariant (SIFT)	87.46	95.72
	Lunula	
Principal component analysis (PCA)	13.62	15.91
Analysis of independent components (AIC)	14.28	14.27
Haar wavelet	14.82	15.90
PCA+Haar	15.39	16.98
AIC+Haar	16.96	18.16
Feature transformation of scale-invariant (SIFT)	17.49	19.14

Using different algorithms, image feature extraction was demonstrated, and using Naive Bayes classifiers and SVM, the accuracy was compared in all the algorithms used, Figure 6 demonstrated the comparison results taken when we used the mentioned algorithms and classifiers. Figure 6(a) showed the results for the nailbed, and Figure 6(b) showed the comparison results for the Lunula. When analyzing the results in Figure 6, the results showed that the Scale-invariant feature, when analyzed using the SVM method, was greater accuracy than all other algorithms used, while the SIFT algorithm showed greater accuracy than other algorithms using both classifiers. When applying the SVM classifier to the SIFT algorithm, it showed an 8% increase compared to the features of the same algorithm when using the Naive Bayes classifier.

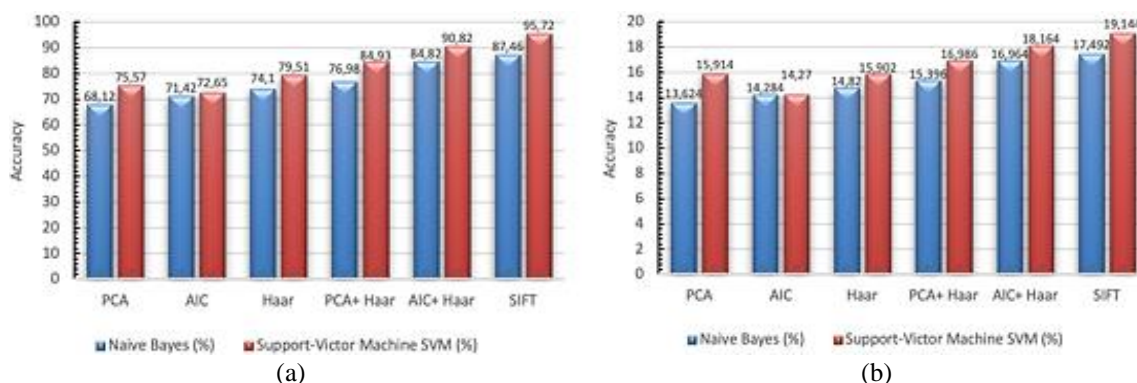


Figure 6. The performance comparison measurements for the accuracy using SVM and Naive Bayes techniques for (a) nail bed and (b) nail Lunula

#### 4. CONCLUSION

This paper proposed a new system for detecting vital identifiers using the nail surface and the lunula of the right thumb of a healthy human hand. In the beginning, we measured the main parameters of the nail, such as nail length and width, the ratio of length to width W/L, and the radius of nail curvature in all the samples that were examined in order to determine the appropriate shape of the nail studied, especially for small-sized images of the nail lunula in order to be used as a primary reference in fingernail prints. We used a set of algorithms to extract the essential basic features, and then we combined these algorithms to reach the highest accuracy in the results. To compare the obtained results, we used two types of classifiers, a Naive Bayes classifier and transformation with a SVM classifier. The results showed that the SIFT algorithm gave the best results in both classifiers used, where the results were higher than the rest of the algorithms used. This study was conducted on 100 participants from one region, and it may be possible in the future to expand this study to more than one region in order to reach more accurate results, especially concerning race, skin color, and age. Although in this research we relied on healthy nails for people who do not suffer from any skin disease or any previous record related to nail diseases, one of the substantial challenges that we must face in future work when using the nail surface for biological identifiers is to overcome the nail polish used, especially when women.




#### REFERENCES

- [1] E. A. Abed, R. J. Mohammed, and D. T. Shihab, "Intelligent multimodal identification system based on local feature fusion between iris and finger vein," *Indonesian Journal of Electrical Engineering and Computer Science*, vol. 21, no. 1, pp. 224–232, Jan. 2021, doi: 10.11591/ijeecs.v21.i1.pp224-232.
- [2] M. El-Beqqal, M. Azizi, and J. L. Lanet, "Multimodal access control system combining RFID, fingerprint and facial recognition," *Indonesian Journal of Electrical Engineering and Computer Science*, vol. 20, no. 1, pp. 405–413, Oct. 2020, doi: 10.11591/ijeecs.v20.i1.pp405-413.
- [3] E. M. Cherrat, R. Alaoui, and H. Bouzahir, "A multimodal biometric identification system based on cascade advanced of fingerprint, finger vein and face images," *Indonesian Journal of Electrical Engineering and Computer Science*, vol. 17, no. 3, p. 1562, Mar. 2020, doi: 10.11591/ijeecs.v17.i3.pp1562-1570.
- [4] O. Munteanu, F. M. Filipoiu, M. M. Cirstoiu, A. I. Băloiu, I. A. Petrescu, and R. E. Bohiltea, "A comprehensive study regarding the intrauterine development of nails," *Organogenesis*, vol. 17, no. 1–2, pp. 14–19, Apr. 2021, doi: 10.1080/15476278.2021.1899739.
- [5] D. Nigam, S. N. Patel, P. M. D. R. Vincent, K. Srinivasan, and S. Arunmozhi, "Biometric authentication for intelligent and privacy-preserving healthcare systems," *Journal of Healthcare Engineering*, vol. 2022, pp. 1–15, Mar. 2022, doi: 10.1155/2022/1789996.
- [6] J. O. Shin *et al.*, "Onychophagia: detailed clinical characteristics," *International Journal of Dermatology*, vol. 61, no. 3, pp. 331–336, Mar. 2022, doi: 10.1111/ijd.15861.
- [7] M. A. A. Maksoud, "Nail-fold excision without matricectomy for treatment of ingrown toe nails," *Al-Azhar Medical Journal*, vol. 47, no. 2, pp. 321–328, Apr. 2018, doi: 10.12816/0052257.
- [8] J. R. Stokes *et al.*, "Should the nail plate be replaced or discarded after nail bed repair in children Nail bed INJury Analysis (NINJA) randomised controlled trial: A health economic and statistical analysis plan," *Trials*, vol. 21, no. 1, p. 833, Dec. 2020, doi: 10.1186/s13063-020-04724-1.
- [9] E. Haneke, "Anatomie, biologie, physiologie und grundzüge der pathologie des nagelorgans," *Hautarzt*, vol. 65, no. 4, pp. 282–290, Apr. 2014, doi: 10.1007/s00105-013-2702-2.
- [10] V. K. Ortner, V. D. Mandel, M. Haedersdal, and P. A. Philipsen, "Impregnation of healthy nail tissue with optical clearing agents for improved optical coherence tomography imaging," *Skin Research and Technology*, vol. 27, no. 2, pp. 178–182, Mar. 2021, doi: 10.1111/srt.12923.
- [11] P. Sihota, R. N. Yadav, V. Dhiman, S. K. Bhadada, V. Mehandia, and N. Kumar, "Investigation of diabetic patient's fingernail quality to monitor type 2 diabetes induced tissue damage," *Scientific Reports*, vol. 9, no. 1, p. 3193, Feb. 2019, doi: 10.1038/s41598-019-39951-3.






- [12] M. Barbosa, T. Brouard, S. Cauchie, and S. M. De-Sousa, "Secure biometric authentication with improved accuracy," in *Lecture Notes in Computer Science (including subseries Lecture Notes in Artificial Intelligence and Lecture Notes in Bioinformatics)*, vol. 5107 LNCS, 2008, pp. 21–36.
- [13] S. Garg, A. Kumar, and M. Hanmandlu, "Biometric authentication using finger nail surface," in *International Conference on Intelligent Systems Design and Applications, ISDA*, Nov. 2012, pp. 497–502, doi: 10.1109/ISDA.2012.6416588.
- [14] G. K. O. Michael, T. Connie, and A. B. J. Teoh, "Touch-less palm print biometrics: Novel design and implementation," *Image and Vision Computing*, vol. 26, no. 12, pp. 1551–1560, Dec. 2008, doi: 10.1016/j.imavis.2008.06.010.
- [15] M. Alghamdi, P. Angelov, and L. P. Alvaro, "Person identification from fingernails and knuckles images using deep learning features and the Bray-Curtis similarity measure," *Neurocomputing*, vol. 513, pp. 83–93, Nov. 2022, doi: 10.1016/j.neucom.2022.09.123.
- [16] P. K. Balasubramanian, W.-C. Lai, G. H. Seng, C. Kavitha, and J. Selvaraj, "APESTNet with mask R-CNN for liver tumor segmentation and classification," *Cancers*, vol. 15, no. 2, p. 330, Jan. 2023, doi: 10.3390/cancers15020330.
- [17] A. Baba, "A Literature survey of Gabor filter and its application New self-maintenance solutions for smart electrical distribution systems View project Deep Learning with Applications," *View project Türk Hava Kurumu Üniversitesi (UTAA)*. 2017, doi: 10.13140/RG.2.2.11079.50085.
- [18] K. M. Jeevan, A. A. B. Gowda, and P. V. Kumar, "An image enhancement method based on gabor filtering in wavelet domain and adaptive histogram equalization," *Indonesian Journal of Electrical Engineering and Computer Science*, vol. 21, no. 1, pp. 146–153, Jan. 2021, doi: 10.11591/ijeecs.v21.i1.pp146-153.
- [19] S. Yelmanov and Y. Romanyshyn, "A new approach to image enhancement based on modified histogram equalization," in *International Scientific and Technical Conference on Computer Sciences and Information Technologies*, Sep. 2019, vol. 1, pp. 5–9, doi: 10.1109/STC-CSIT.2019.8929838.
- [20] W. S. Alazawee, Z. H. Naji, and W. T. Ali, "Analyzing and detecting hemorrhagic and ischemic stroke-based on bit plane slicing and edge detection algorithms," *Indonesian Journal of Electrical Engineering and Computer Science*, vol. 25, no. 2, pp. 1003–1010, Feb. 2022, doi: 10.11591/ijeecs.v25.i2.pp1003-1010.
- [21] M. Kachroudi, "Revisiting indirect ontology alignment: New challenging issues in cross-lingual context." pp. 1–14, 2021, doi: 10.48550/arXiv.2104.01628.
- [22] J. Su, J. Meng, W. Hou, R. Wang, and X. Luo, "Multi-angle optical image automatic registration by combining point and line features," *Sensors*, vol. 22, no. 3, p. 739, Jan. 2022, doi: 10.3390/s22030739.
- [23] O. Bchir, M. M. B. Ismail, and H. Aljam, "Region-based image retrieval using relevance feature weights," *International Journal of Fuzzy Logic and Intelligent Systems*, vol. 18, no. 1, pp. 65–77, Mar. 2018, doi: 10.5391/IJFIS.2018.18.1.65.
- [24] B. G. Ballé and J. V. Sos, "Configurations of points and topology of real line arrangements," *Mathematische Annalen*, vol. 374, no. 1–2, pp. 1–35, Jun. 2019, doi: 10.1007/s00208-018-1673-0.
- [25] T. H. Nguyen and B. V. Ngo, "ROI-based features for classification of skin diseases using a multi-layer neural network," *Indonesian Journal of Electrical Engineering and Computer Science*, vol. 23, no. 1, pp. 216–228, Jul. 2021, doi: 10.11591/ijeecs.v23.i1.pp216-228.
- [26] P. Basu and P. R. Cohen, "Macrolunula: Case reports of patients with trauma-associated enlarged lunula and a concise review of this nail finding," *Cureus*, Jul. 2018, doi: 10.7759/cureus.2998.
- [27] M. Kamate, G. P. Prashanth, and S. Gandhi, "A boy with sapphire thumbnails: Lunulae ceruleae," *Indian Journal of Pediatrics*, vol. 81, no. 7, pp. 737–738, Jul. 2014, doi: 10.1007/s12098-014-1341-7.
- [28] J. V. Stone, *Independent component analysis*. The MIT Press, 2018.
- [29] M. Wolter, F. Blanke, R. Heese, and J. Garcke, "Wavelet-packets for deepfake image analysis and detection," *Machine Learning*, vol. 111, no. 11, pp. 4295–4327, Nov. 2022, doi: 10.1007/s10994-022-06225-5.
- [30] S. Khan, S. Nazir, A. Hussain, A. Ali, and A. Ullah, "An efficient JPEG image compression based on Haar wavelet transform, discrete cosine transform, and run length encoding techniques for advanced manufacturing processes," *Measurement and Control (United Kingdom)*, vol. 52, no. 9–10, pp. 1532–1544, Nov. 2019, doi: 10.1177/0020294019877508.
- [31] M. Ahsan, K. S. Haq, X. Liu, S. A. Lone, and M. Nisar, "A Haar wavelets based approximation for nonlinear inverse problems influenced by unknown heat source," *Mathematical Methods in the Applied Sciences*, vol. 46, no. 2, pp. 2475–2487, Jan. 2023, doi: 10.1002/mma.8655.
- [32] A. Tharwat, "Independent component analysis: An introduction," *Applied Computing and Informatics*, vol. 17, no. 2, pp. 222–249, Apr. 2018, doi: 10.1016/j.aci.2018.08.006.
- [33] T. Akutsu *et al.*, "Application of independent component analysis to the iKAGRA data," *Progress of Theoretical and Experimental Physics*, vol. 2020, no. 5, May 2020, doi: 10.1093/ptep/ptaa056.
- [34] H. V. Elst, "Tutorial on principal component analysis, with applications in R." 2021, doi: 10.13140/RG.2.2.20075.16168/2.
- [35] Y. Lu, A. A. Liu, and Y. T. Su, "Mitosis detection in biomedical images," in *Computer Vision for Microscopy Image Analysis*, Elsevier, 2020, pp. 131–157.
- [36] K. Sakuma *et al.*, "Wearable nail deformation sensing for behavioral and biomechanical monitoring and human-computer interaction," *Scientific Reports*, vol. 8, no. 1, p. 18031, Dec. 2018, doi: 10.1038/s41598-018-36834-x.
- [37] H. E. Kim, N. S. Kim, and W. H. Do, "Classification of adult women's fingernail type," *Fashion & Textile Research Journal*, vol. 22, no. 4, pp. 504–514, Aug. 2020, doi: 10.5805/sfti.2020.22.4.504.
- [38] B. Gaye, D. Zhang, and A. Wulamu, "Improvement of support vector machine algorithm in big data background," *Mathematical Problems in Engineering*, vol. 2021, pp. 1–9, Jun. 2021, doi: 10.1155/2021/5594899.
- [39] T. N. Viet, H. Le Minh, L. C. Hieu, and T. H. Anh, "The naïve bayes algorithm for learning data analytics," *Indian Journal of Computer Science and Engineering*, vol. 12, no. 4, pp. 1038–1043, Aug. 2021, doi: 10.21817/indjcs/2021/v12i4/211204191.




**BIOGRAPHIES OF AUTHORS**

**Tahani Ghanim Al-Sultan**    she graduated from the Technical Engineering College of Mosul/Northren Technical University/Iraq in 2000 and obtained a Bachelor's degree in Medical Instrumentation Engineering, and in 2020 she obtained a Master's degree in Medical Electronic Instrumentation Techniques Engineering from the Middle Technical University. A faculty member at the Northern Technical University since 2002, lecturer in department of medical equipment technology engineering. Her interests are in Biomedical, electronics, deep learning, signal processing, medical instruments, and image processing. She can be contacted via the official email: tahaniAl-sultan@ntu.edu.iq.






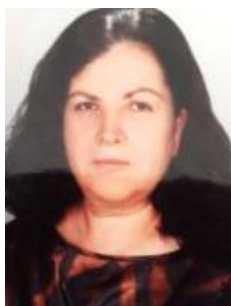
**Aza Qays Abduljabar**    she graduated from the Technical Engineering College of Mosul/Northren Technical University/Iraq in 2005 and obtained a bachelor's degree in medical Instrumentation Engineering, and in 2021 she obtained a master's degree in medical electronic Instrumentation Techniques Engineering from the Middle Technical University. A faculty member at the Northern Technical University since 2006. Her interests are in Biomedical, electronics, deep learning, signal processing, medical instruments, image processing, and she has several published research papers in those field. She can be contacted via the official email: azzakays@ntu.edu.iq.






**Warqaa Hashim Alkhaled**    she graduated from the Technical Engineering College of Mosul/Northren Technical University/Iraq in 2005 and obtained a bachelor's degree in medical Instrumentation Engineering, and in 2020 she obtained a master's degree in medical electronic Instrumentation Techniques Engineering from the Middle Technical University. A faculty member at the Northern Technical University since 2006. Her interests are in biomedical, electronics, deep learning, signal processing, medical instruments, image processing, and she has several published research papers in those field. She can be contacted via the official email: warqaahasim@ntu.edu.iq.



**Zaid Husham Al-Sawaff**    received the technical bachelor's degree in medical instrumentation technology from the Northern Technical University, Iraq. The M.Sc. degree in Biomedical Engineering from Osmania University, India 2015. in the present time, he got his Ph.D. in Biomedical Engineering from Kastamonu University, Turkey 2022. He is currently a lecturer with the Department of Medical Instrumentation Technology, Technical College, Northern Technical University, Mosul-IRAQ. he has supervised many B. Scs and M.Sc. students in Kastamonu University. His research interests include medical instrumentation, biomedical engineering, computational chemistry, and nanotechnology. He can be contacted by email: zaidalsawaff@ntu.edu.iq.



**Fatma Kandemirli**    obtained her Ph.D. at Gebze High Technology Institute, Chemistry Department, in 1999. In 2005-2010 Associate Professor, Department of Chemistry, University of Kocaeli, Kocaeli, Turkey. In 2010-2012 Professor, Department of Chemistry, University of Niğde, Niğde, Turkey. In 2012 Professor, Department of Biomedical Engineering, University of Kastamonu, Kastamonu. Dr. Kandemirli's activities and interests are Synthesis of inorganic compounds, QSAR, reaction mechanism, quantum chemical calculations, quantum chemical calculations of corrosion inhibitors. She can be contacted by email: fkandemirli@yahoo.com.